Phase Composition and Disorder in $La_2(Sn,Ti)_2O_7$ Ceramics: New Insights from NMR Crystallography

Arantxa Fernandes, David McKay, Scott Sneddon, Daniel M. Dawson, Sebastian Lawson, Richard Veazey, Karl R. Whittle and Sharon E. Ashbrook,

Supporting Information

S1. Proposed structural models for $La_2Ti_2O_7$

Figure S1.1 shows the orthorhombic structural model of $La_2Ti_2O_7$ proposed by Scheunemann (**C**).[S1] The monoclinic proposed by Gasperin[S2] (**B**) is shown in Figure 1b of the main text. The unit cell parameters for the two models are compared in Table S1.1.

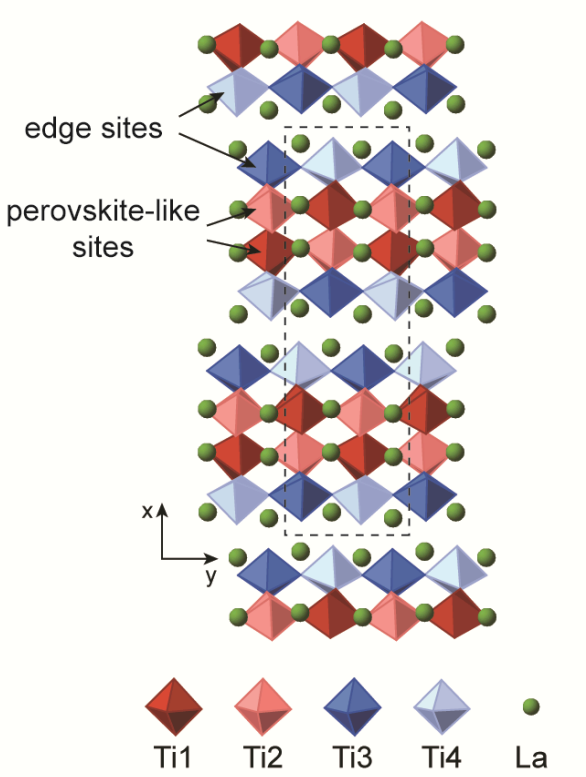

Figure S1.1 Orthorhombic structure of $La_2Ti_2O_7$ proposed by Scheunemann,[S1] with numbering reflecting that of the monoclinic structure (see main text, Figure 1). The dashed line indicates the unit cell.

Table S1.1 Unit cell parameters for the structural models of $La_2Ti_2O_7$ considered in this work. **B**, **B**^{SC} and **C**.

Model	ICSD code	Space group	a / Å	b / Å	c / Å	α (°)	β (°)	γ (°)
B[S2]	4132	$P2_1$	7.8	13.011	5.546	90.0	98.6	90.0
C[S1]	1950	$Pna2_1$	25.745	7.81	5.547	90.0	90.0	90.0

S2. Powder XRD patterns of $La_2(Sn,Ti)_2O_7$

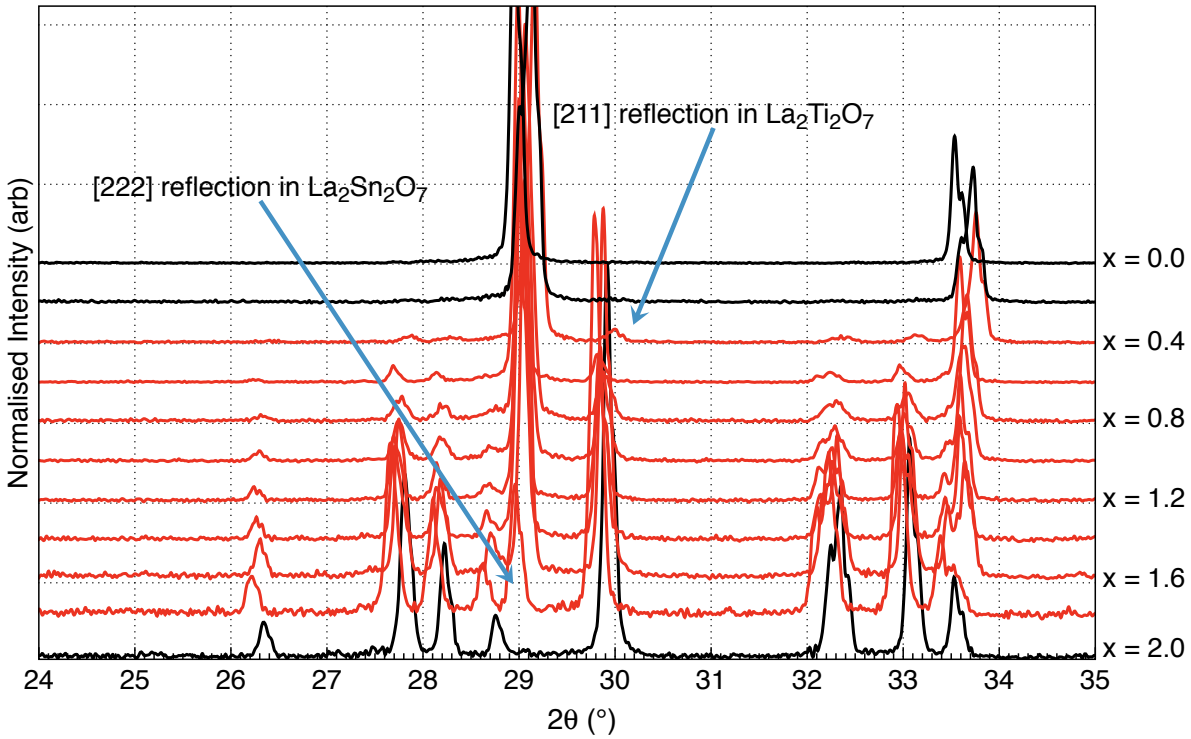

Figure S2.1 Normalised X-ray diffraction patterns for the whole compositional range of $La_2Sn_{2-x}Ti_xO_7$. The arrows indicate the first evidence of the [222] reflection (the strongest) in the stannate-rich pyrochlore, and the [211] reflection (the strongest) in $La_2Ti_2O_7$.

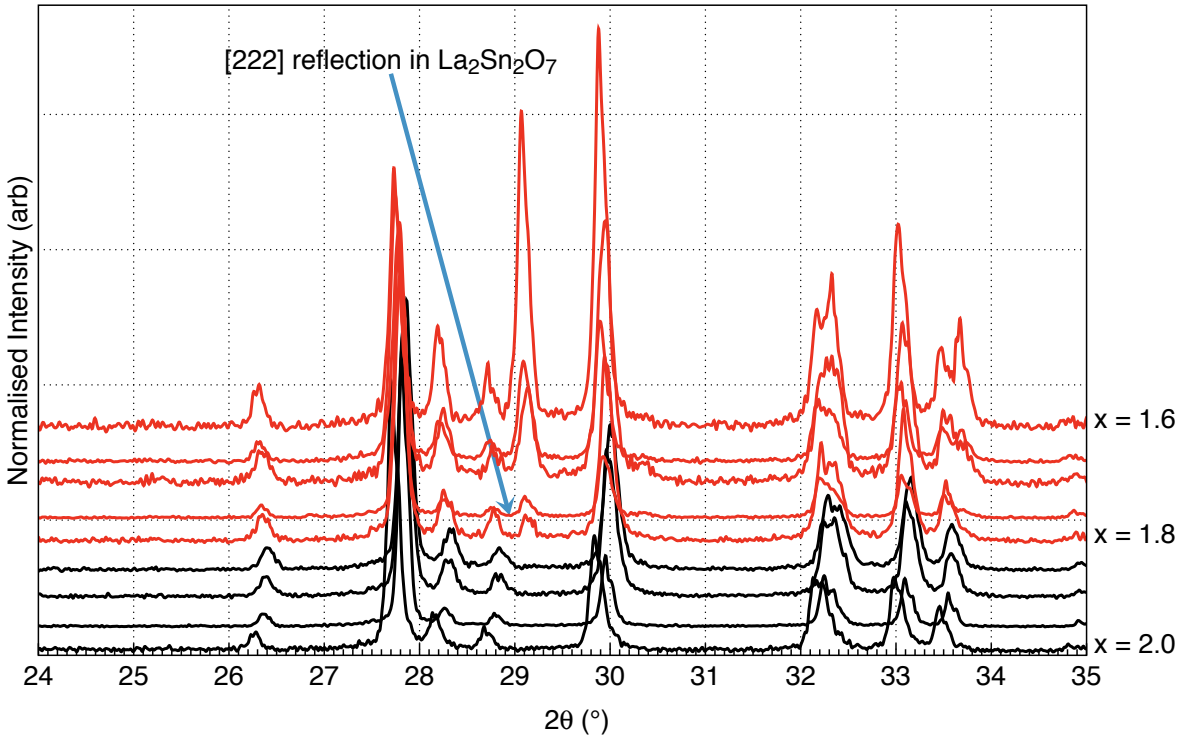

Figure S2.2 Normalised X-ray diffraction patterns for $La_2Sn_{2-x}Ti_xO_7$, where x = 2 to 1.6, *i.e.*, Ti-rich compositions. The arrow indicates the first evidence of the [222] reflection (the strongest) in the stannate-rich pyrochlore.

S3. ^{119}Sn slow MAS and CSA-amplified PASS spectra

Figure S3.1 shows a ^{119}Sn slow MAS NMR spectrum of $La_2Sn_2O_7$, acquired at B_0 = 9.4 T with an MAS rate of 2 kHz. Analytical lineshape fitting gives δ_{iso} = –642 ppm, Ω = 43 (5) ppm and κ = –0.93 (5).

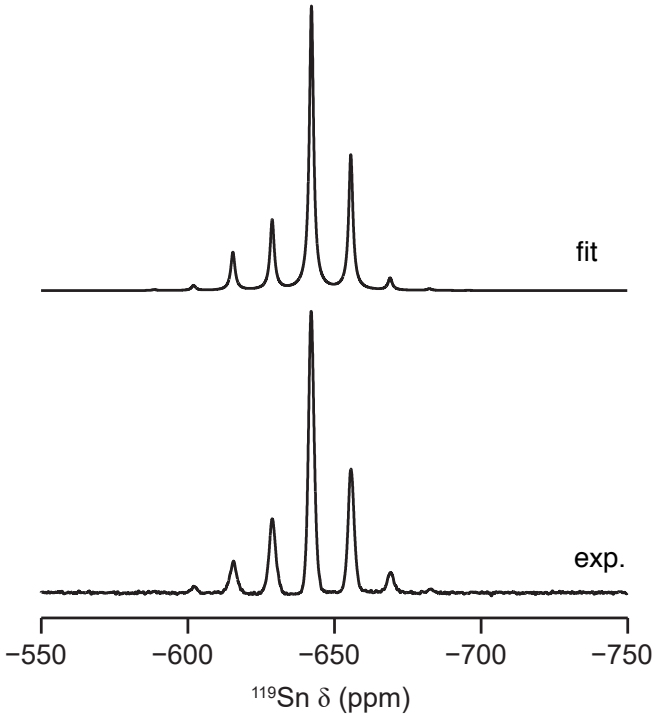

Figure S3.1 ^{119}Sn (9.4 T, 2 kHz MAS) NMR spectrum of $La_2Sn_2O_7$.

For samples with Ti substitution it is difficult to measure the CSA parameters using a slow MAS spectrum, owing to the presence of more than one resonance and CSA-amplified PASS experiments were employed. The experiments were carried out at an MAS rate of 10 kHz, with a total scaling factor, $N_T = (n_{PASS} + 1)N$, of 6.67, resulting in an apparent MAS rate of 1.5 kHz in the indirect dimension. Spectra were acquired using the pulse sequence shown in Figure S3.2, by averaging between 78 and 182 transients for each of 16 rows, with a recycle interval of 30 s. Fitting of the sideband patterns in the indirect dimension was carried out using SIMPSON,[S3] by comparison to a one-dimensional MAS

spectrum (assuming ideal pulses). The root-mean-square (rms) error quoted is that outputted by SIMPSON, as described in the SIMPSON manual.[S3]

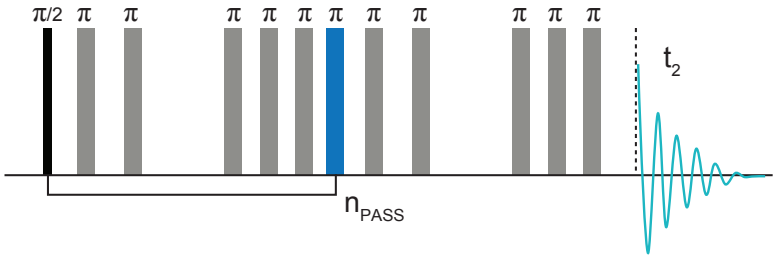

Figure S3.2 Pulse sequence used for CSA-amplified PASS experiments.[S4,S5] Cogwheel phase cycling is employed to reduce the length of the phase cycle.[S6] The scaling factor (N) is determined by the timings of the 5-π pulses and higher total scaling factors (N_T) can be utilised through concatenation of the pulse blocks, with $N_T = (n_{PASS} + 1)N$.

Figure S3.3 shows two-dimensional CSA-amplified PASS spectra of $La_2Sn_{1.8}Ti_{0.2}O_7$, $La_2Sn_{1.6}Ti_{0.4}O_7$ and $La_2Sn_{1.4}Ti_{0.6}O_7$, along with the fitting of the sideband manifolds extracted for each site and contour plots of the rms deviation. The values of δ_{iso}, Ω and κ extracted from the spectra are given in Table S3.1.

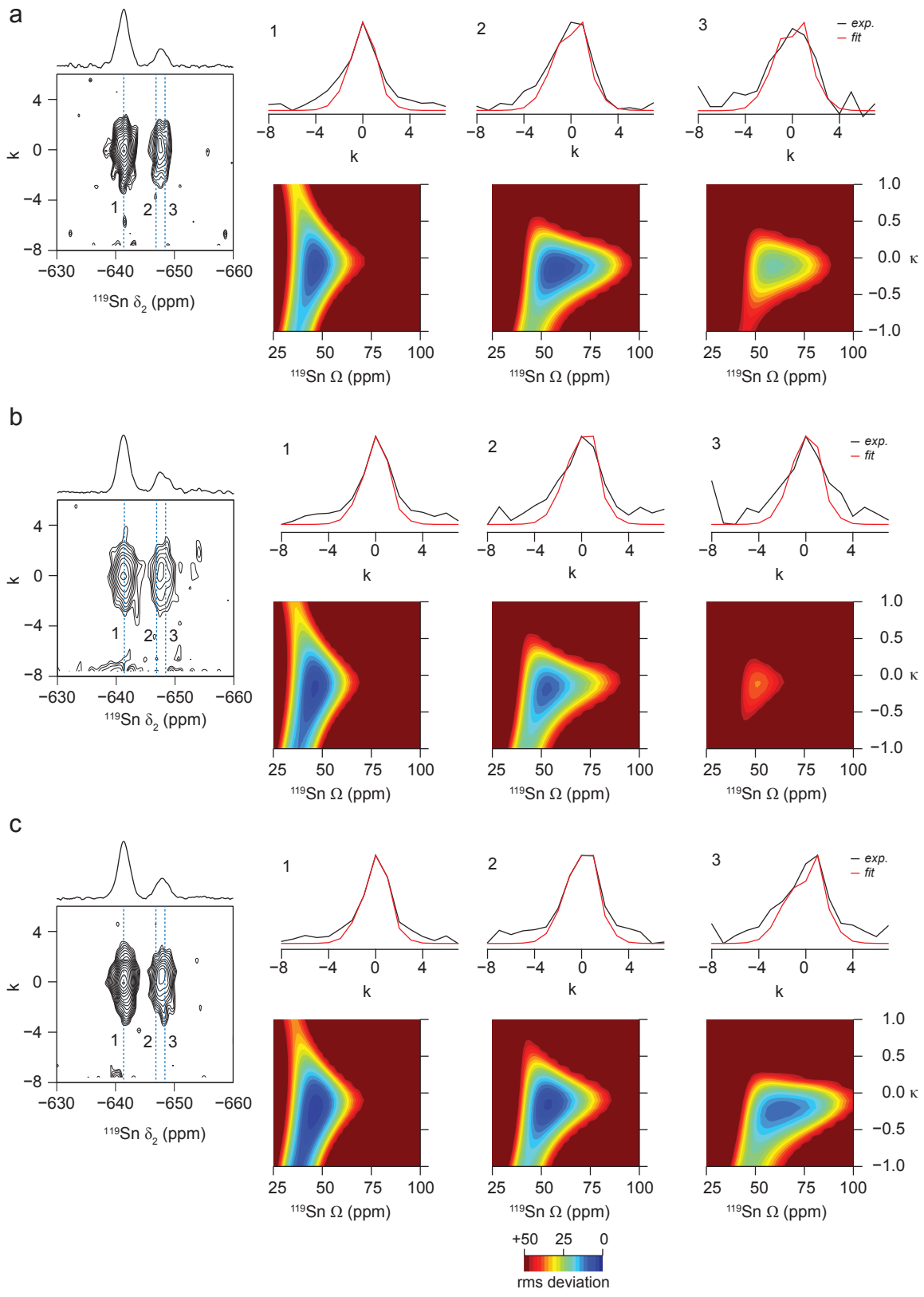

Figure S3.3 ^{119}Sn (9.4 T) 2D CSA-amplified PASS NMR spectra, extracted spinning sideband manifolds (black line), fittings (red line), and contour plots of the rms deviation (arbitrarily cut at 50) for (a) $La_2Sn_{1.8}Ti_{0.2}O_7$, (b) $La_2Sn_{1.6}Ti_{0.4}O_7$, and (c) $La_2Sn_{1.4}Ti_{0.6}O_7$. The MAS rate was 10 kHz and $N_T = 6.67$.

Table S3.1. Experimental ^{119}Sn NMR δ_{iso}, Ω, κ and corresponding rms error deviation extracted from the spinning sideband manifolds from the 2D CSA-amplified PASS spectra of $La_2Sn_{1.8}Ti_{0.2}O_7$, $La_2Sn_{1.6}Ti_{0.4}O_7$ and $La_2Sn_{1.4}Ti_{0.6}O_7$ in Figure S3.3. The next-nearest neighbour (NNN) environment is also shown.

Sample	δ_{iso} (ppm)	Ω (ppm)	κ	rms error	NNN
$La_2Sn_{1.8}Ti_{0.2}O_7$					
	−641.4	46.6 ± 2.5	−0.12 ± 0.2	6.68	Sn6
	−647.1	57.7 ± 3.9	−0.15 ± 0.1	6.16	Sn5Ti
	−648.5	59.5 ± 4.5	−0.11 ± 0.1	20.67	Sn5Ti
$La_2Sn_{1.6}Ti_{0.4}O_7$					
	−641.2	46.3 ± 2.5	−0.17 ± 0.2	4.18	Sn6
	−647.1	53.1 ± 3.1	−0.18 ± 0.1	9.07	Sn5Ti
	−648.5	51.1 ± 3.0	−0.12 ± 0.1	35.82	Sn5Ti
$La_2Sn_{1.4}Ti_{0.6}O_7$					
	−641.4	46.5 ± 2.5	−0.22 ± 0.2	2.41	Sn6
	−647.4	53.6 ± 2.9	−0.15 ± 0.1	4.26	Sn5Ti
	−648.3	62.2 ± 6.1	−0.23 ± 0.1	10.07	Sn5Ti

S4. DFT calculations

Ti substitution into $La_2Sn_2O_7$

As shown in Figure S4.1, the B site in the pyrochlore structure has 6 B-site next nearest neighbours (NNN). Calculations were performed for a single unit cell of $La_2Sn_2O_7$, where the environment of one of the Sn species was modified systematically, altering both the number of the surrounding B-site cations (*i.e.*, Sn and Ti) and their spatial arrangement, as shown in Figure S1.1(b). In each case, the geometry of the structure was optimized (with atomic coordinates and unit cell parameters allowed to vary), prior to calculation of the NMR parameters.

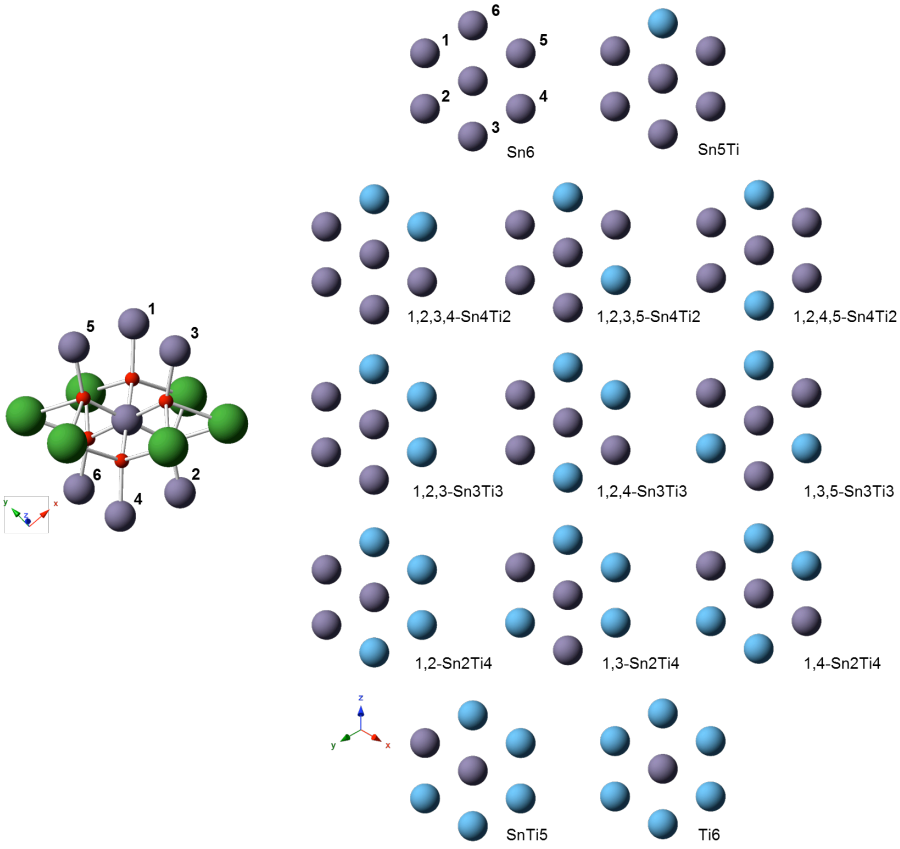

Figure S4.1 Cluster showing the local environment around the six-coordinate B site in the pyrochlore structure. Red spheres denote O, green spheres denote La, and purple spheres denote Sn B site cations. Also shown are possible arrangements of Sn and Ti (blue) on the six NNN B sites that surround the central Sn B site, viewed down the [111] lattice direction with O and La sites omitted for clarity.

Sn substitution into $La_2Ti_2O_7$

Table S4.1 shows the calculated Sn NMR shifts for models based on a supercell of (monoclinic)[S2] $La_2Ti_2O_7$ with the substitution of two Sn atoms (giving a doping level of 12.5%).

Table S4.1. Computed ^{119}Sn shifts for double Sn substitutions into $\mathbf{B}^{SC}$ showing Sn···Sn distances and relative enthalpies (ΔH) for each model. Sn^A and Sn^B are arbitrary labels for two inserted Sn atoms, where numbers denote the position and prime (′) denotes second nearest site of that type.

Sn^A	Sn^B	δ(Sn^A) (ppm)	δ(Sn^B) (ppm)	r(Sn^A–Sn^B) / Å	ΔH / eV
Sn1	Sn1	−594	−594	7.899	0.03
Sn1	Sn1′	−604	−604	4.184	−0.22
Sn1	Sn2	−587	−581	4.054	−0.10
Sn1	Sn2′	−594	−589	5.786	−0.16
Sn1	Sn3	−610	−603	3.832	−0.16
Sn1	Sn3′	−597	−607	5.726	−0.07
Sn1	Sn4	−599	−626	5.459	−0.02
Sn1	Sn4′	−592	−619	5.485	−0.03
Sn2	Sn2	−584	−584	7.899	0.00
Sn2	Sn2′	−598	−598	4.222	−0.24
Sn2	Sn3	−588	−614	5.407	−0.10
Sn2	Sn3′	−584	−604	5.459	−0.07
Sn2	Sn4	−611	−614	3.825	−0.16
Sn2	Sn4′	−587	−615	5.811	−0.01

Sn3	Sn3	−610	−610	7.853	0.09
Sn3	Sn3′	−607	−607	6.013	−0.01
Sn3	Sn4	−607	−615	5.985	0.06
Sn3	Sn4′	−605	−620	3.904	0.05
Sn4	Sn4	−620	−620	7.866	0.23
Sn4	Sn4′	−621	−621	5.983	0.11

S5. Spectral analysis

From the relative intensities of the pyrochlore peaks, it is possible to determine the proportion of Sn/Ti in this phase. Once this is known, this information can be combined with the relative proportion of Sn and Ti in the initial synthesis, and the relative intensities of the peaks attributed to pyrochlore and layered perovskite phases, respectively, to determine both the composition of the layered perovskite phase and the relative proportion of each phase in the sample. Two approaches have been considered in this work.

Method I

Taking as an example the sample synthesised with equal molar ratios of Sn and Ti (*i.e.*, formally La_2SnTiO_7), the three pyrochlore peaks in the ^{119}Sn MAS spectrum have relative intensities of 61.6%, 34.4% and 4.0% (Sn4Ti2). If we can assume that we have 6 B site NNN, 6 are Sn for the first peak, 5 Sn and 1 Ti for the second and 4 Sn 2 Ti for the third, then of 600 surrounding B site cations $(61.6 \times 6) + (34.4 \times 5) + (4.0 \times 4) = 557.5$ are Sn and 42.5 are Ti. This gives 92.9% and 7.1% Sn and Ti on the B sites in the pyrochlore phase, and a composition of $La_2Sn_{1.86}Ti_{0.14}O_7$.

From the ^{119}Sn MAS spectrum 87.7% of the Sn in the starting mixture is found in the pyrochlore phase, and 12.3% in a layered perovskite phase. For an initial composition of La_2SnTiO_7 for every 200 B site cations, 100 would be Sn and 100 would be Ti. Of the 100 Sn atoms in the starting mixture we know that 87.7 (*i.e.*, 87.7%) are found in the pyrochlore phase and 12.3 (*i.e.*, 12.3%) in the layered perovskite phase. To determine the number of the 100 initial Ti atoms that appear in the final pyrochlore phase we multiply the Ti/Sn ratio in that phase by the 87.7 Sn atoms that are present, *i.e.*, $(0.14/1.86) \times 87.7 = 6.7$. The remaining 93.3 Ti atoms must then be in the layered perovskite phase. From here we know that there are 87.7 Sn and 6.7 Ti atoms in the pyrochlore phase (confirming we have 92.9%

Sn and 7.1% Ti (*i.e.*, $La_2Sn_{1.86}Ti_{0.14}O_7$) and by analogy we have 12.3 Sn and 93.3 Ti atoms in the layered perovskite phase, demonstrating that has 11.6% Sn and 88.4% Ti, giving a formula of $La_2Sn_{0.23}Ti_{1.77}O_7$.

The relative proportions of pyrochlore and layered perovskite phases can be determined by considering the % of the total B site cations found in the two phases, *i.e.*, (87.7 + 6.7) in the pyrochlore phase and (12.3 + 93.3) in the layered perovskite. This gives (94.4/200) = 47.2% pyrochlore and (105.6/200) = 52.8% layered perovskite. Therefore, when x = 1 the sample is a two phase mixture of 47.2% of a pyrochlore phase with composition $La_2Sn_{1.86}Ti_{0.14}O_7$ and 52.8% layered perovskite with composition $La_2Sn_{0.23}Ti_{1.77}O_7$.

Method II

In this approach it is assumed that there is a random distribution of B site cations, and that the relative intensity of the peak at ~ –641 ppm can be assigned entirely to sites with 6 Sn NNN. From simple statistics, the probability, P, of finding n Sn NNN is given by

$$P(n\ Sn\ NNN) = Z\,(1 - x/2)^n\,(x/2)^{6-n}\ , \qquad (S5.1)$$

where x is defined by the formula ($La_2Sn_{2-x}Ti_xO_7$) and Z is the number of possible permutations for arranging n atoms on 6 sites. For the case of 6 Sn NNN, $P = 1\,(1 - x/2)^{6,}$ and so x can be determined directly from the relative intensity (expressed as a fraction) of the peak assigned 6 Sn NNN. For the example above, this accounted for 61.6% of the pyrochlore intensity giving x = 0.155 and a formula of $La_2Sn_{1.85}Ti_{0.15}O_7$ in contrast to the $La_2Sn_{1.86}Ti_{0.14}O_7$ obtained previously. Once this formula is known the analysis is identical to that described above and gives for the example discussed a material composed of 47.5% of a pyrochlore phase with composition $La_2Sn_{1.85}Ti_{0.15}O_7$ and 52.5% layered perovskite with composition $La_2Sn_{0.24}Ti_{1.76}O_7$. This is in very good agreement with the results obtained

using method I, validating the approaches used and suggesting that the low number of Ti cations in the pyrochlore phase are, indeed, distributed randomly. A comparison of the relative proportions of each phase present (and their compositions) determined using the two approaches is shown in Figure S5.1 for all compositions in the series.

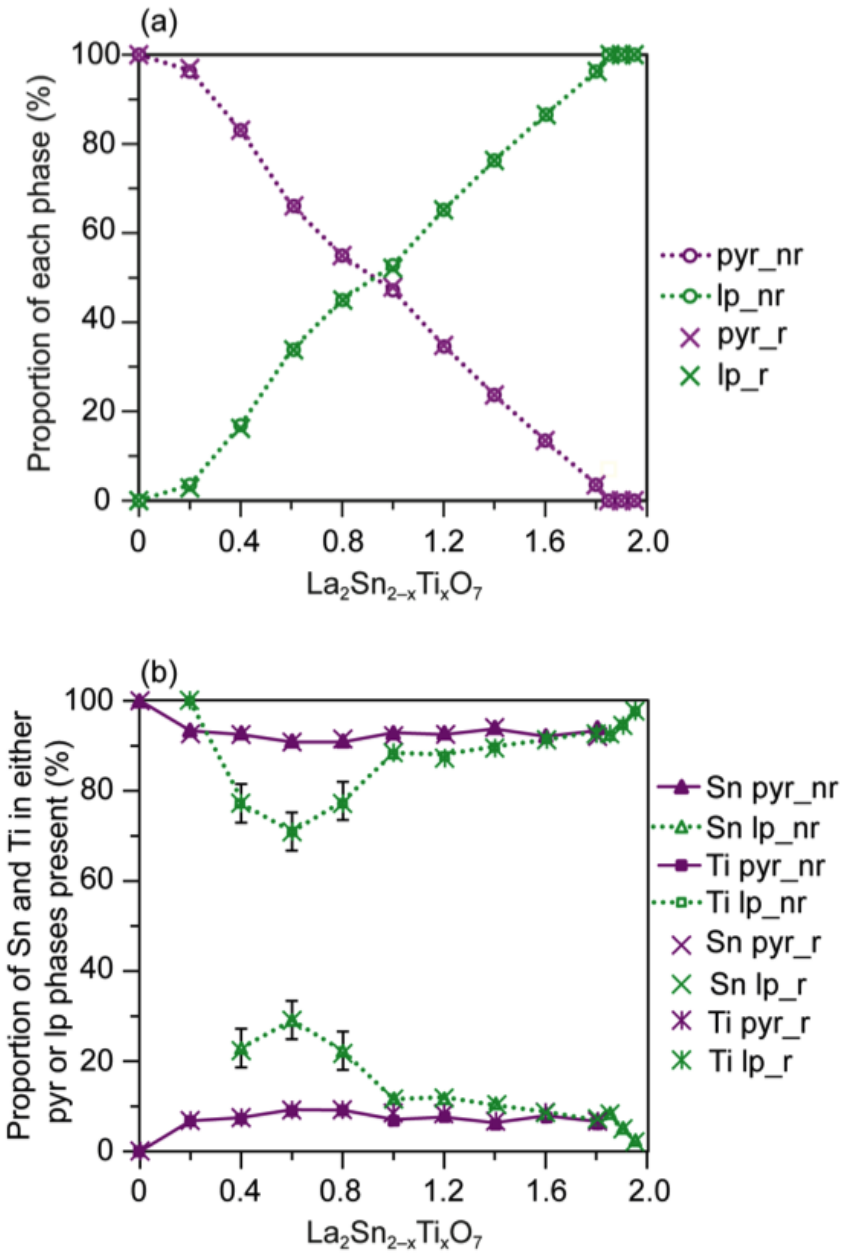

Figure S5.1 Comparison of (a) the relative proportions of the pyrochlore and layered perovskite phases present (expressed as a %) and (b) their composition (expressed as a % of Sn and Ti), calculated using methods I (nr) and II (r) discussed above. In method II, a random distribution of the B site cations is assumed.

S6. References

S1. Scheunemann, K.; Mueller-Buschbaum, H. B. Zur Kristallstruktur von $La_2Ti_2O_7$. *J. Inorg. Nucl. Chem.*, **1975**, *37*, 1879-1881.

S2. Gasperin, P. R. Dititanate de Lanthane. *Acta Cryst.* **1975**, *B31*, 2129-2130.

S3. (a) Bak, M.; Rasmussen, J.; Nielsen, N. SIMPSON: a General Simulation Program for Solid-State NMR Spectroscopy. *J. Magn. Reson.* **2000**, *147*, 296-330. (b) http://nmr.au.dk/software/simpson/.

S4. Orr, R. M.; Duer, M. J.; Ashbrook, S. E. Correlating Fast and Slow Chemical Shift Spinning Sideband Patterns in Solid-State NMR. *J. Magn. Reson.* **2005**, *174*, 301-309.

S5. Orr, R. M.; Duer, M.; *J.* Applications of the CSA-Amplified PASS Experiment. *Solid State Nucl. Magn. Reson.* **2006**, *30*, 1-8.

S6. (a) Levitt, M. H.; Madhu, P. K.; Hughes, C. E. Cogwheel Phase Cycling. *J. Magn. Reson*. 2002, *155*, 300-306. (b) Ivchenko, N.; Hughes, C. E.; Levitt, M. H. Application of Cogwheel Phase Cycling to Sideband Manipulation Experiments in Solid-State NMR. *J. Magn. Reson.* **2003**, *164*, 286-293.